J Mater Sci (2010) 45:6634–6642
DOI 10.1007/s10853-010-4754-3

Experimental investigation and thermodynamic calculation of phase equilibria in the In–Sb–Zn ternary system

Duško Minić · Jelena Đokić · Dragan Manasijević · Dejan Čikara · Dragana Živković · Nadežda Talijan

Received: 25 January 2010 / Accepted: 8 July 2010 / Published online: 20 July 2010

Abstract Binary thermodynamic data, successfully used for phase diagram calculations of binary systems In–Sb, In–Zn, and Sb–Zn, were used for prediction of phase equilibria in ternary In–Sb–Zn system. The liquidus projection, invariant equilibria and several vertical sections were calculated using the CALPHAD method. Alloys, situated along three calculated vertical sections, were investigated by differential thermal analysis (DTA). The experimentally determined phase transition temperatures were compared with predicted results. Phase identification of selected samples was done using scanning electron microscopy (SEM) with energy dispersive X-ray microanalysis (EDS).

Introduction

Scientific interest in phase relationships in the In–Sb–Zn system is mainly due to two reasons. The first one is a potential application in semiconductor industry. The second one is the development of Pb-free solders.

In this paper, the phase transition temperatures of the In–Sb–Zn ternary system were investigated using differential thermal analysis (DTA). Experimentally determined phase transition temperatures were compared with the results of thermodynamic binary-based prediction, based on the 4.4 SGTE values of Gibbs energies for pure elements [1] and thermodynamic binary data included in the COST 531 thermodynamic database [2].

D. Minić (✉) · J. Đokić · D. Čikara
Faculty of Technical Sciences, University of Pristina,
38220 Kosovska Mitrovica, Serbia
e-mail: dminic65@nadlanu.com

D. Manasijević · D. Živković
Technical Faculty, University of Belgrade, VJ 12,
19210 Bor, Serbia

N. Talijan
Technology and Metallurgy, Institute of Chemistry,
Belgrade, Serbia

Experimental procedure

All samples were prepared from pure elements (purity higher than 99.99%) supplied by Alfa Aesar, Karlsruhe, Germany. Weighed amounts of the materials were melted in a resistance furnace under argon atmosphere and melts were held as liquids for several hours to assure homogeneity. Homogenized samples were equilibrated at 100 °C (below the lowest invariant temperature in the constitutive binaries) for 2 months and quenched in the water with ice.

Differential thermal analysis (DTA) experiments were made using a laboratory-made DTA apparatus with the thermocouples inserted directly into the sample and inert reference material under following conditions: flowing argon atmosphere, sample masses about 2 g, and alumina as the reference material. A heating rate of 5 °C/min was employed both for calibration and measurement of the prepared samples. The data were collected using the personal computer. Microstructure investigations were done using scanning electron microscopy (SEM, JEOL JSM 6460) with energy dispersive X-ray microanalysis (EDS, Oxford Instruments).

Thermodynamic models and crystallographic data

The phase diagram of the In–Sb–Zn ternary system was calculated using the Calculation of Phase Diagrams

(CALPHAD) method [3, 4], based on the optimized thermodynamic parameters for constitutive binary systems only. The basic mathematical method used for the calculation of phase equilibria is a constrained minimization of Gibbs energy for a given temperature, pressure and overall composition. This approach is common for all currently available software packages for the modeling of thermodynamic properties and phase diagrams of multi component systems.

The molar Gibbs energy of a phase ϕ can be considered as the sum of a number of different contributions:

$$G_{\mathrm{m}}^{\phi} = G_{\mathrm{ref}}^{\phi} + G_{\mathrm{id}}^{\phi} + G_{\mathrm{E}}^{\phi} + G_{\mathrm{mag}}^{\phi} + G_{\mathrm{P}}^{\phi} + \cdots \quad (1)$$

where G_{ref}^{ϕ} is the weighted sum of the molar Gibbs energy of the system constituents i (elements, species, compounds etc.) of the phase ϕ relative to the chosen reference state (typically the stable element reference state—SER),

$$G_{\mathrm{ref}}^{\phi} = \sum_{i=1}^{n} x_i \cdot {}^{\mathrm{o}}G_i^{\phi} \quad (2)$$

and its temperature dependence is given by

$$G(T) = a + bT + cT\ln(T) + \sum_i d_i T^n \quad (3)$$

where a–d_i are adjustable coefficients.

There is also a contribution to the Gibbs energy from ideal random mixing of the constituents on the crystal lattice, denoted G_{id}^{ϕ},

$$G_{\mathrm{id}}^{\phi} = RT\sum_{i=1}^{n} x_i \cdot \ln(x_i), \quad i = 1, \ldots, n \quad (4)$$

for an n-constituent system.

G_{E}^{ϕ} is the excess Gibbs energy, which describes the influence of non-ideal mixing behavior on the thermodynamic properties of a solution phase and is given by the Muggianu extension of the Redlich–Kister formalism [5, 6]

$$G_{\mathrm{E}}^{\varphi} = \sum_{\substack{i,j=1 \\ i\neq j}}^{n} x_i x_j \sum_{z=0}^{m} {}^{z}L\left(x_i - x_j\right)^{z} + \sum_{\substack{i,j,k=1 \\ i\neq j\neq k}}^{n} x_i x_j x_k L_{ijk} \quad z = 0, \ldots, m \quad (5)$$

where the interaction parameters, describing the mutual interaction among constituents i and j, are denoted as ${}^{z}L$. The liquid phase and solid solution phases are modeled in this way, but more complex phases, such as intermetallic compounds, are usually modeled using the compound energy

Table 1 Considered phases, their crystallographic data and database names [11]

Phase name	Common name	Pearson symbol
LIQUID	Liquid	
TETRAG_A6	(In)	*tI*2
ZINCBLENDE_B3	αInSb	*cF*8
RHOMBO_A7	(Sb)	*hR*2
HCP_ZN	(Zn)	*hP*2
SBZN_BETA	β	*oP*16
SBZN_GAMMA	γ	…
SBZN_DELTA	δ	(*a*)
SBZN_EPSILON	ε	(*a*)
SBZN_ZETA	ζ	*oI**
SBZN_ETA	η	*oP*30

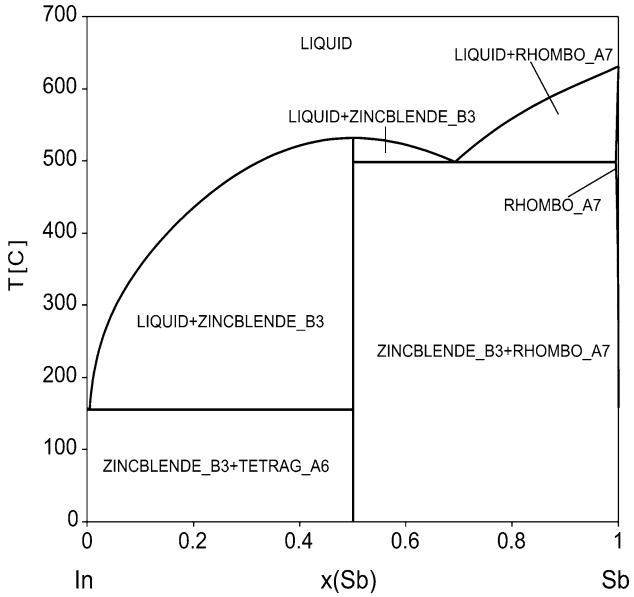

Fig. 1 Calculated phase diagram of the In–Sb binary system

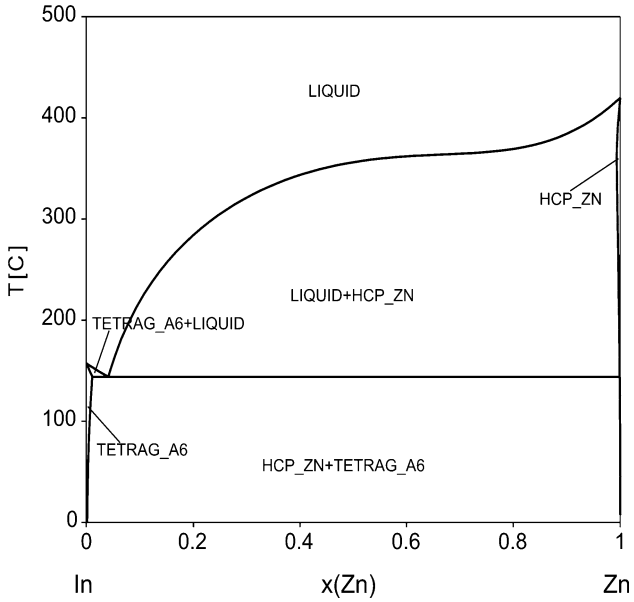

Fig. 2 Calculated phase diagram of the In–Zn binary system

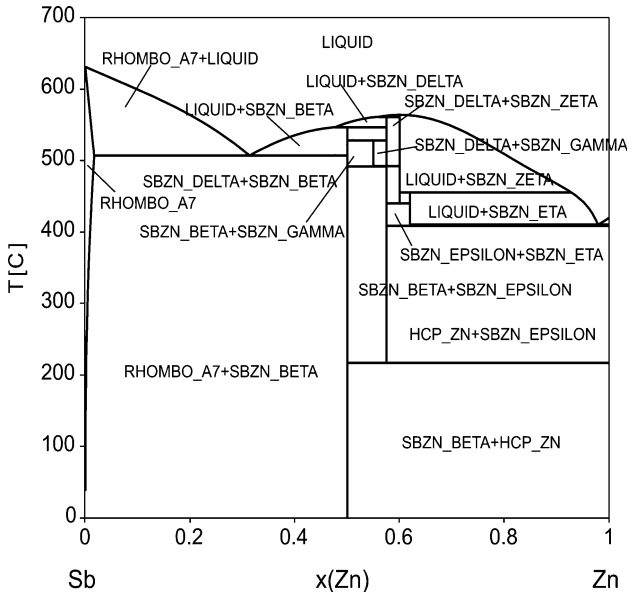

Fig. 3 Calculated phase diagram of the Sb–Zn binary system

formalism [7]. Additional terms may be necessary for the proper description of the Gibbs energy from Eq. 1. G^{ϕ}_{mag} in Eq. 1 is the magnetic contribution and G^{ϕ}_{P} is the pressure term. The Version 4.4 of the SGTE Unary Database (Scientific Group Thermodata Europe) of Gibbs energies for stable and metastable states of pure elements, compiled by Dinsdale [1], was used. Thermodynamic data for the In–Sb system were taken from Ref. [8], for the In–Zn system were published in Ref. [9], and thermodynamic data for the system Sb–Zn were taken from Ref. [10]. All this data are included in the COST 531 Database for Lead Free Solders [2].

The phases from constitutive binary subsystems considered for thermodynamic binary-based prediction with their crystallographic data are listed in Table 1.

Literature data

Binary systems

In–Sb system

The original data for the In–Sb system from Anderson were reported by Ansara et al. [8] and referred to as a private communication. Small modification to data for the original α-InSb phase was made [2]. The phase was remodeled and renamed to ZINCBLENDE_B3 [2] to provide compatibility with general model for the crystallographic structure of this phase. A calculated phase diagram of the In–Sb binary system is shown in Fig. 1.

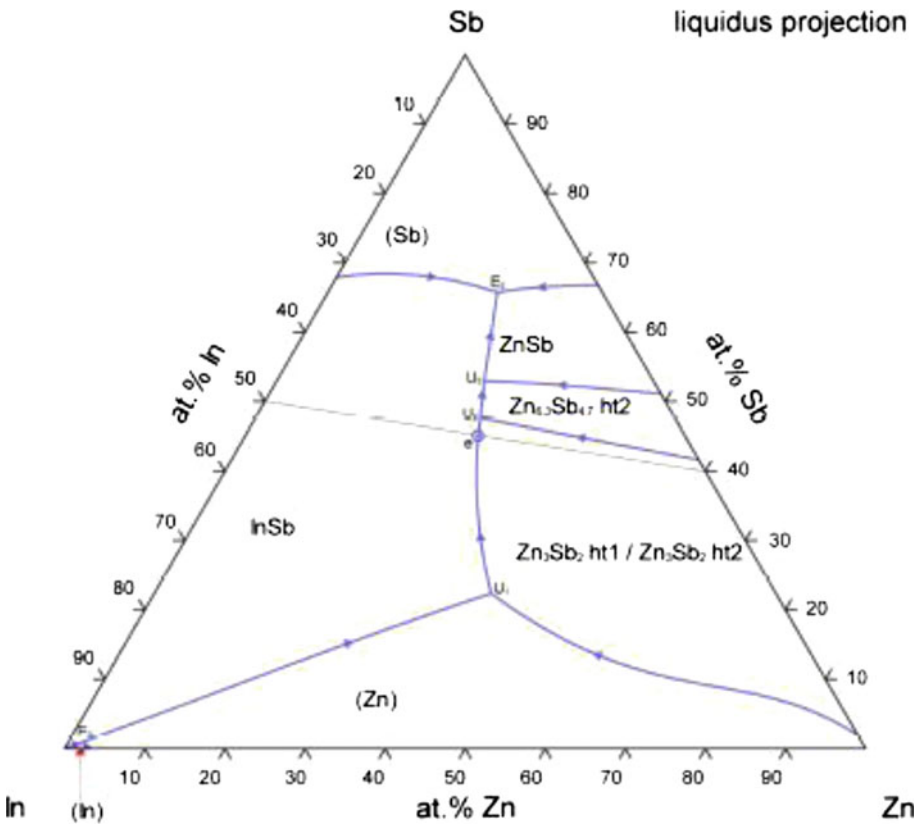

Fig. 4 Liquidus projection of the In–Sb–Zn ternary system from [13]

Table 2 Optimized thermodynamic parameters for constitutive binaries used in this study

Optimized thermodynamic parameters	References
LIQUID-CONSTITUENTS: IN, SB, ZN	
L(LIQUID,IN,SB;0) 298.15 −25631.2 + 102.9324 * T − 13.45816 * T * LN(T)	[8]
L(LIQUID,IN,SB;1) 298.15 −2115.4 − 1.31907 * T	[8]
L(LIQUID,IN,SB;2) 298.15 2908.9	[8]
L(LIQUID,IN,ZN;0) 298.15 12401 − 4.4498 * T	[9]
L(LIQUID,IN,ZN;1) 298.15 −3186 + 1.756 * T	[9]
L(LIQUID,IN,ZN;2) 298.15 679	[9]
L(LIQUID,SB,ZN;0) 298.15 −11740.942 − 0.1283 * T	[10]
L(LIQUID,SB,ZN;1) 298.15 -427.582-0.809855*T	[10]
L(LIQUID,SB,ZN;2) 298.15 34440.943 − 33.59286 * T	[10]
TETRAG_A6 CONSTITUENTS: IN, ZN	
L(TETRAG_A6,IN,ZN;0) +4430 − 4.4498 * T	[9]
L(TETRAG_A6,IN,ZN;1) = 9717	
RHOMBO_A7 CONSTITUENTS: IN, SB, ZN	
L(RHOMBO_A7,IN,SB;0) = + 15 * T	[8]
L(RHOMBO_A7,IN,ZN;0) = 3500	[2]
L(RHOMBO_A7,SB,ZN;0) = 0.0	[10]
ZINCEBLENDE_B3 2 SUBLATTICES, SITES .5: .5 CONSTITUENTS: IN:SB	
G(ZINCBLENDE_B3,IN:SB;0)-0.5 H298(TETRAG_A6,IN;0)-0.5 H298(RHOMBO_A7,SB;0) = −16411.1 + .81674 * T + 1.293581 * T * LN(T) +.5*GHSERIN + .5*GHSERSB	[2]
HCP_ZN 2 SUBLATTICES, SITES 1: .5 CONSTITUENTS: IN,ZN : VA	
L(HCP_ZN,IN,ZN:VA;0) = 23114	[9]
BETA_SBZN - 2 SUBLATTICES, SITES 0.5: 0.5, CONSTITUENTS: SB:ZN	
G(BETA_SBZN,SB:ZN;0)-0.5 H298(RHOMBOHEDRAL_A7,SB;0)-0.5 H298(HCP_A3,ZN;0) = −11542.68 + 5 * T + 0.5 * GHSERZN + 0.5 * GHSERSB	[10]
GAMMA_SBZN - 2 SUBLATTICES, SITES 0.45: 0.55, CONSTITUENTS: SB:ZN	
GAMMA_SBZN,SB:ZN;0)-0.45 H298(RHOMBOHEDRAL_A7,SB;0)-0.55 H298(HCP_A3,ZN;0) = −8748.7632 + 1.3365 * T + 0.45 * GHSERSB + 0.55 * GHSERZN	[10]
EPSILON_SBZN - 2 SUBLATTICES, SITES 0.425: 0.575, CONSTITUENTS: SB:ZN	
G(EPSILON_SBZN,SB:ZN;0)-0.425 H298(RHOMBOHEDRAL_A7,SB;0)-0.575	[10]
H298(HCP_A3,ZN;0) = −7730.454 + 0.425 * GHSERSB + 0.575 * GHSERZN	
DELTA_SBZN - 2 SUBLATTICES, SITES 0.425: 0.575, CONSTITUENTS: SB:ZN	
G(DELTA_SBZN,SB:ZN;0)-0.425 H298(RHOMBOHEDRAL_A7,SB;0)-0.575	[10]
H298(HCP_A3,ZN;0) = −7348 − 0.5 * T + 0.425 * GHSERSB + 0.575 * GHSERZN	
ZETA_SBZN - 2 SUBLATTICES, SITES 0.4: 0.6, CONSTITUENTS: SB:ZN	
G(ZETA_SBZN,SB:ZN;0)-0.4 H298(RHOMBOHEDRAL_A7,SB;0)-0.6 H298(HCP_A3,ZN;0) = −4918.01 − 3.37557 * T + 0.4 * GHSERSB + 0.6 * GHSERZN	[10]
ETA_SBZN - 2 SUBLATTICES, SITES 0.38: 0.62, CONSTITUENTS: SB : ZN	
G(ETA_SBZN,SB:ZN;0)-0.38 H298(RHOMBOHEDRAL_A7,SB;0)-0.62 H298(HCP_A3, ZN;0) = −5042.71 − 2.743826*T + 0.38 * GHSERSB + 0.62 * GHSERZN	[10]

In–Zn system

The data from the critical assessment of Lee [9] were included in the COST 531 database [2] and used in this study. A calculated phase diagram of the In–Zn binary system is shown in Fig. 2.

Sb–Zn system

The data for the Sb–Zn system included in Ref. [2] and used in this work are from the critical assessment of Liu et al. [10]. The authors obtained good agreement between calculated and experimental values for a wide range of properties. A calculated phase diagram of the Sb–Zn binary system is shown in Fig. 3.

In–Sb–Zn ternary system

The ternary system In–Sb–Zn was investigated by Skudnova et al. [12]. Based on their results the liquidus projection of this ternary system was published by [13] and shown in Fig. 4. Presented liquidus projection include seven primary crystalization regions. Six larger regions ((Zn), (Sb), $Zn_{6,3}Sb_{4,7}$ht2, Zn_3Sb_2ht1/Zn_3Sb_2ht2, InSb and ZnSb) and one smaller region (In). The existance of five invariant reactions with two of them E-type and three of them U-type were reported. The ternary In–Sb–Zn system and solubility of Zn in indium antimonide (InSb) at 480 °C were investigated by Lapkina et al. [14]. The maximum solubility of Zn in InSb was found to be 1.51 at.% .

Results and discussion

Existing experimental thermodynamic data for the liquid phase from the literature and thermal analysis data from this study were compared with calculation results based on thermodynamic parameter dataset given in Table 2.

Predicted liquidus projection of the In–Sb–Zn system

Based on thermodynamic parameter values given in Table 2, the liquidus projection of the In–Sb–Zn ternary system is calculated and plotted in Fig. 5. Ten invariant reactions and 10 primary crystallization regions

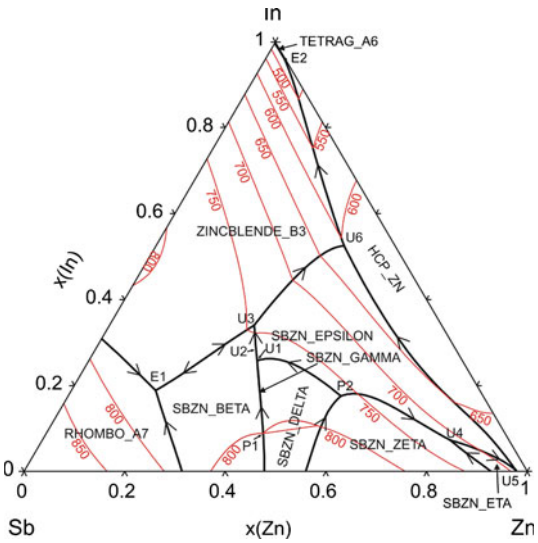

Fig. 5 The predicted liquidus projection of the In–Sb–Zn ternary system

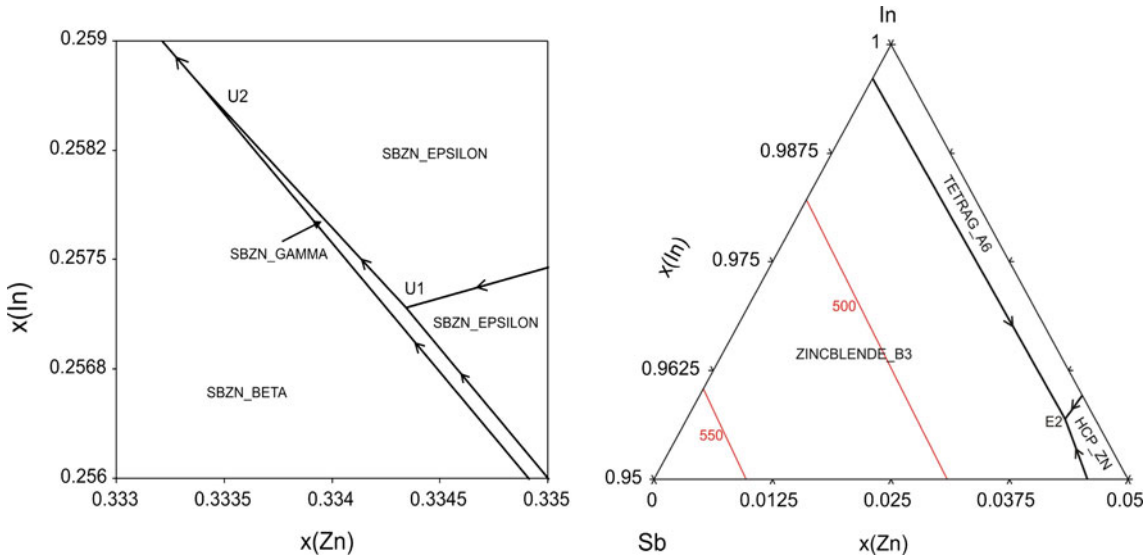

Fig. 6 Magnified views of the liquidus projection of the In–Sb–Zn ternary system in the composition regions close to the: **a** U1 and U2 points; **b** E2 ternary eutectic point

(RHOMBO_A7, HCP_ZN, TETRAG_A6, ZINCEBLENDE_B3, SBZN_BETA, very narrow SBZN_GAMMA, SBZN_DELTA, SBZN_ZETA, SBZN_EPSILON, SBZN_ETA) are predicted in this ternary system. Magnified views of the liquidus projection of the In–Sb–Zn ternary system in the vicinity of the calculated E2, U1, and U2 invariant points are shown in Fig. 6.

The predicted invariant reactions in ternary In–Sb–Zn system are listed in Table 3, as well as the reaction temperatures and the types of those invariant reactions. It can be seen that in ternary In–Sb–Zn system there are 10 predicted invariant reactions: two of them are ternary eutectic reactions (E-type reactions), five liquid transition reactions (U-type reactions), and three of them are peritectic reactions (P-type reactions).

Experimental study of phase transition temperatures

In order to experimentally study phase transition temperatures of the In–Sb–Zn ternary system, the alloys with overall compositions alongside three chosen vertical sections with molar ratio In:Zn = 1, Sb:Zn = 1 and vertical section with the constant Zn ratio (x(Zn) = 0.2) were investigated using DTA. The analysis of DTA measurements was performed during the heating of samples. Predicted phase diagrams were used as help to interpret obtained DTA results (Table 4).

From the DTA results, three invariant reactions have been identified. They correspond to predicted reactions E1, E2, and U5 given in Table 3.

Table 3 Predicted invariant reaction of ternary In–Sb–Zn system

T (°C)	Reaction	Type	Composition		
			x(In)	x(Sb)	x(Zn)
527.86	LIQUID + SBZN_DELTA + SBZN_BETA → SBZN_GAMMA	P1	0.083	0.484	0.433
491.76	LIQUID + SBZN_ZETA + SBZN_DELTA → SBZN_EPSILON	P2	0.175	0.283	0.542
491.76	LIQUID + SBZN_DELTA + SBZN_GAMMA → SBZN_EPSILON	P3	0.257	0.408	0.335
491.41	LIQUID + SBZN_GAMMA → SBZN_BETA + SBZN_EPSILON	U1	0.259	0.408	0.333
472.07	LIQUID + SBZN_BETA → ZINCBLENDE_B3 + SBZN_EPSILON	U2	0.339	0.374	0.287
469.5	LIQUID → RHOMBO_A7 + SBZN_BETA + ZINCBLENDE_B3	E1	0.188	0.645	0.167
439.49	LIQUID + SBZN_ZETA → SBZN_EPSILON + SBZN_ETA	U3	0.072	0.117	0.811
408.16	LIQUID + SBZN_ETA → SBZN_EPSILON + HCP_ZN	U4	0.004	0.022	0.974
329.66	LIQUID + SBZN_EPSILON → ZINCBLENDE_B3 + HCP_ZN	U5	0.525	0.102	0.373
142.33	LIQUID → ZINCBLENDE_B3 + HCP_ZN + TETRAG_A6	E2	0.957	0.003	0.040

Table 4 DTA results for the investigated alloys of the In–Sb–Zn ternary system

Sample composition (at.%)	Phase transition temperature [°C]		
	Invariant reaction	Other transition	Liquidus
Sb10In45Zn45	155.9; 312.1	–	343.2
Sb25In37.5Zn37.5	140.1; 319.4	411.6	463.1
Sb30In35Zn35	144.1; 317.1	394.3	472.2
Sb80In10Zn10	470.8	–	549.3
In10Sb70Zn20	472.2	–	514.7
In30Sb50Zn20	466.9	–	491.7
In40Sb40Zn20	143.1; 308.9	429.7	496.1
In50Sb30Zn20	146.6; 315.5	394.5	472.2
In70Sb10Zn20	138	311.6	343.6
In20Sb40Zn40	213.8; 326.5	–	499.4
In40Sb30Zn30	143.6; 323.7	–	458.5
In60Sb20Zn20	142.5	309.5	412.7
In80Sb10Zn10	140.8	226.2	330.1

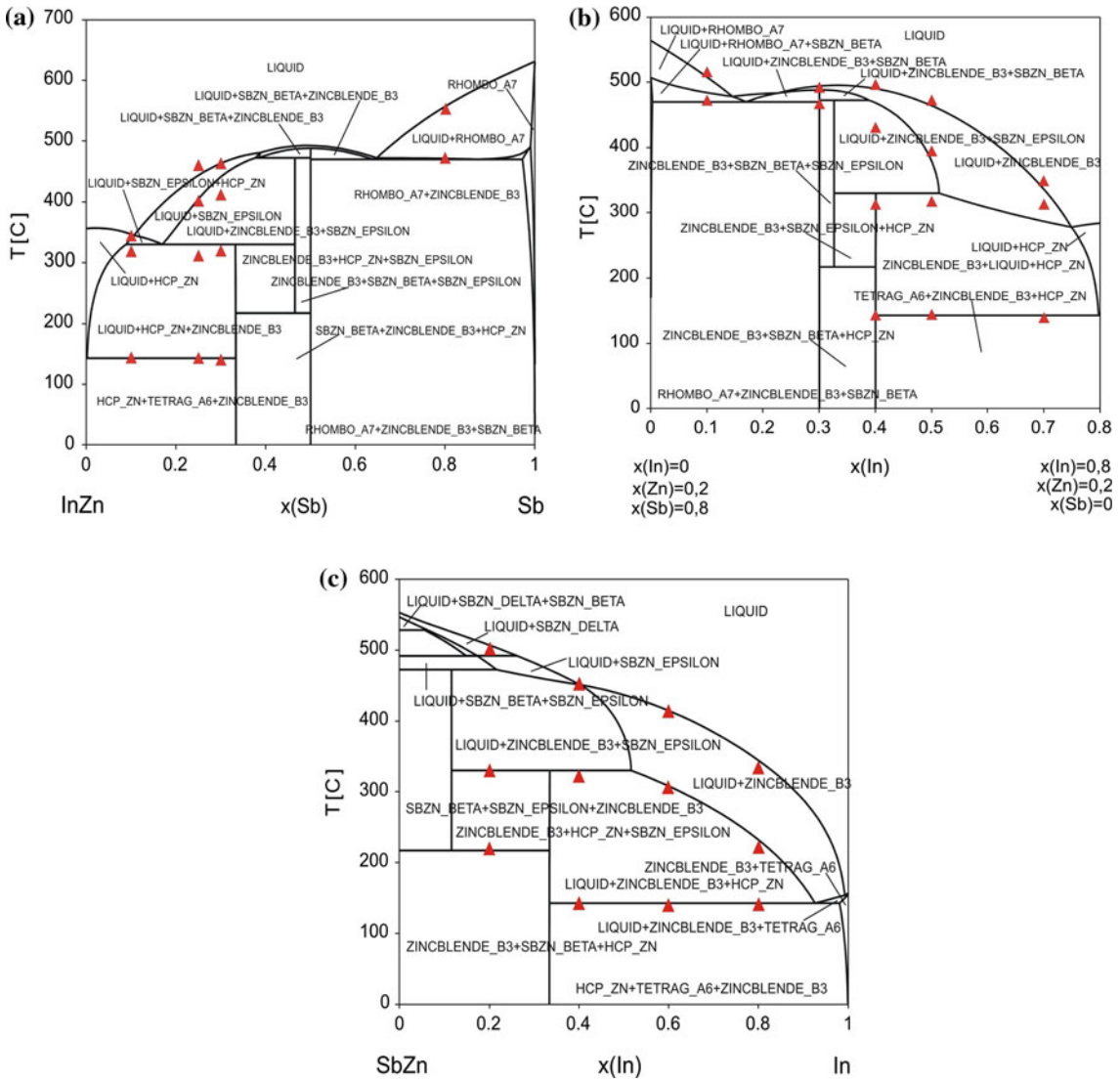

Fig. 7 Calculated vertical sections of the In–Sb–Zn ternary system compared with DTA results from the present study: **a** In:Zn = 1; **b** x(Zn) = 0.2, **c** Sb:Zn = 1

Predicted phase diagrams of vertical sections with phase transition temperatures from the present DTA measurements are plotted in Fig. 7.

The example of DTA heating curve for the sample Sb30In35Zn35 is presented in Fig. 8. The first detected peak at 144.1 °C is associated with appearance of predicted ternary eutectic reaction (E2) and the temperature of the second peak at 319 °C is somewhat lower than corresponding temperature of predicted quasi-peritectic reaction (U5). The third peak at 394.3 °C is related with the crystallization of ZINCBLENDE_B3 phase and the fourth peak at 472.2 °C is related with the crossing of liquidus line.

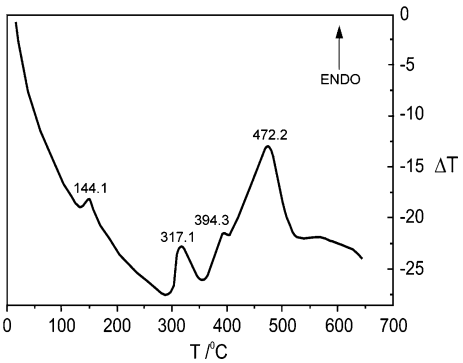

Fig. 8 DTA heating curve for the sample Sb30In35Zn35

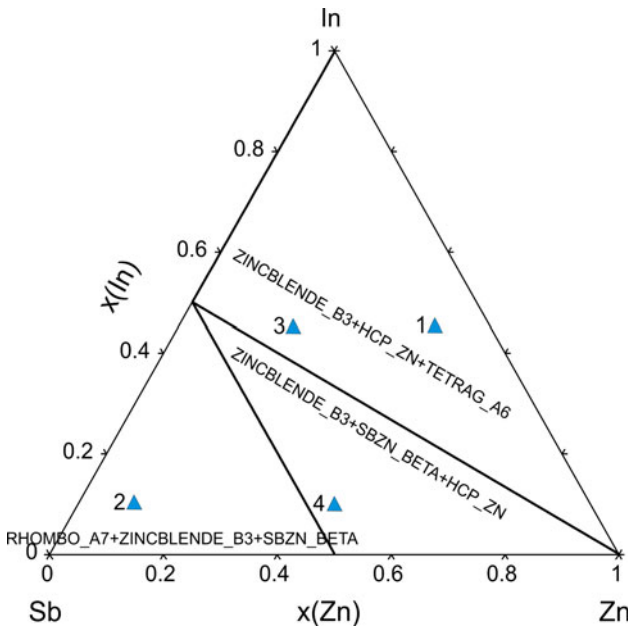

Fig. 9 Isothermal section in ternary In–Sb–Zn systema at 25 °C

Phase identification of selected alloys of the ternary In–Sb–Zn system

Microstructures were investigated for four alloys with the following compositions: Sample 1 was with equal molar ratio of In and Zn, and $x(\mathrm{Sb}) = 0.1$, Sample 2 was also with equal molar ratio of In and Zn and molar ratio of Sb was 0.8. The third sample was with molar ratios $x(\mathrm{In}) = 0.45$, $x(\mathrm{Sb}) = 0.35$ and molar ratio of Zn was 0.2 and Sample 4 had equal molar ratios for Sb and Zn with $x(\mathrm{In}) = 0.1$.

Isothermal section of the ternary In–Sb–Zn system at 25 °C was calculated. Calculated section was plotted on Fig. 9, and compositions with microstructure investigations were marked. There are three-three-phase regions observed in Fig. 10 ((SBZN_BETA + ZINCBLENDE_B3 + HCP_ZN), (TETRAG_A6 + ZINCBLENDE_B3 + HCP_ZN) and (SBZN_BETA + ZINCBLENDE_B3 + RHOMBO_A7)).

Microstructures of the investigated alloys were presented in Fig. 10. Based on investigated compositions of each existing phase in the microstructures for all four alloys, and existing phases in calculated isothermal section at 25 °C a good agreement between experimentally determined and calculated phases can be noticed.

Conclusion

Phase diagram of the ternary In–Sb–Zn system was extrapolated using the CALPHAD method, based on

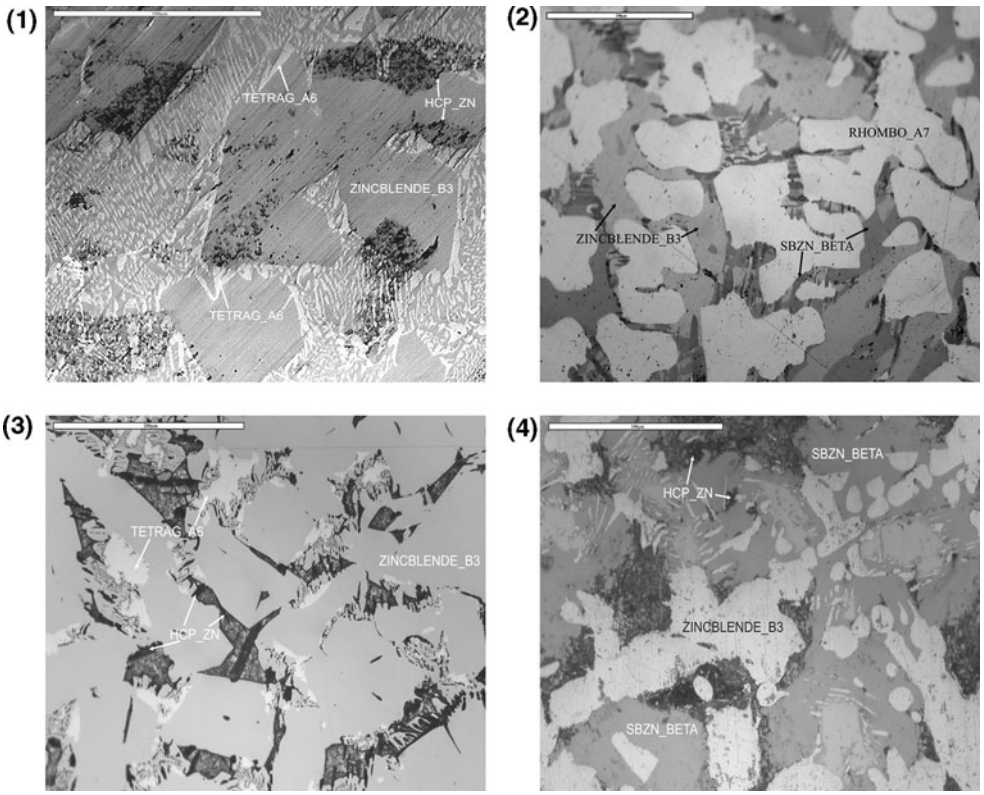

Fig. 10 Microstructures of the investigated alloys

optimized thermodynamic parameters for the boundary binary systems. The calculated liquidus projection and invariant equilibria of the In–Sb–Zn ternary system were presented. Phase transition temperatures of the alloys along three characteristic vertical sections were measured by DTA. Three invariant reactions were identified by DTA results from this study. Calculated melting temperatures are in agreement with thermal analysis results. The phases found in microstructures of investigated alloys are corresponding with the phases in calculated isothermal section at 25 °C.

Acknowledgement This work was supported by Ministry of Science of the Republic of Serbia (Project No. 142043 and 142035B). Calculations were performed by PANDAT 8.1 software.

References

1. Dinsdale AT (2002) SGTE Unary Database, Version 4.4, 2002, www.sgte.org
2. Dinsdale AT, Kroupa A, Vízdal J, Vrestal J, Watson A, Zemanova A (2008) COST 531 Database for Lead-free Solders, Ver. 3.0
3. Saunders N, Miodownik AP (1998) CALPHAD (A comprehensive guide). Elsevier, London
4. Lukas HL, Fries SG, Sundman B (2007) Computational thermodynamics: CALPHAD method. Cambridge University Press, Cambridge, UK
5. Redlich O, Kister A (1948) Ind Eng Chem 40:345
6. Muggianu Y-M, Gambino M, Bros J-P (1975) J Chim Phys 72:83
7. Andersson J-O, Fernandez-Guillermet A, Hillert M, Jansson B, Sundman B (1986) Acta Metall 34:437
8. Ansara I, Chatillon C, Lukas HL, Nishizawa T, Ohtani H, Ishida K, Hillert M, Sundman B, Argent BB, Watson A, Chart TG, Anderson T (1994) CALPHAD 18:177
9. Lee BJ (1996) CALPHAD 20(4):471
10. Liu XJ, Wang CP, Ohnuma I, Kainuma R, Ishida K (2000) J Phase Equilib 21(5):432
11. Dinsdale AT, Kroupa A, Vizdal J, Vrestal J, Watson A, Zemanova A (2008) COST Action 531—atlas of lead free soldering, vol 1. COST Office, Brussels, Belgium
12. Skudnova EV, Karaseva TP, Mirgalovskaya MS (1964) Russ J Inorg Chem 9:201
13. ASM Alloy Phase Diagrams Center. doi:10.1361/apd-in-sb-zn-1401196
14. Lapkina IA, Sorokina OV, Voloshin AE, Shcherbovskii EY, Viryasova TB (1987) Inorg Mater 23:473